

Catalytic Behavior of Rare-Earth Sulfates: Applications in Organic Hydrogenation and Oxidation Reactions

Concepción Cascales,* Berta Gomez Lor, Enrique Gutiérrez Puebla, Marta Iglesias, M. Angeles Monge, Caridad Ruíz Valero, and Natalia Snejko

Instituto de Ciencia de Materiales de Madrid, ICMM, Consejo Superior de Investigaciones Científicas CSIC, Cantoblanco, E-28049 Madrid, Spain

Received April 22, 2004

Two isostructural ammonium rare-earth R double sulfate monohydrates $\text{NH}_4\text{R}(\text{SO}_4)_2 \cdot \text{H}_2\text{O}$, $\text{R} = \text{Y}, \text{Ho}$, have been hydrothermally synthesized at 170 °C for 1 week. The crystal structures established by single-crystal X-ray diffraction are monoclinic, space group $P2_1/n$, $Z = 4$, with unit cell parameters $a = 10.2171(7)$ and $10.219(2)$ Å, $b = 8.3349(5)$ and $8.338(1)$ Å, and $c = 10.3267(7)$ and $10.323(2)$ Å, and $\beta = 119.5290(10)$ and $119.482(3)^\circ$, for $\text{R} = \text{Y}$ and Ho , respectively. The most interesting feature of the 3D structure is the existence of helical channels along the a direction, where isolated RO_8 polyhedra alternate with the two kinds of sulfate groups, and the ammonium cations are located inside the channels. Their infrared and thermal stability analyses have also been performed. These materials behave as active catalysts in hydrogenation reactions of olefins and nitroaromatics, and in highly chemoselective, hydrogen peroxide mediated, oxidation of organic sulfides. High yielding, mild conditions of reactions, suitability for solid-phase reactions, and reusability with no detriment of selectivity, activity, or yield are among the advantages of these described solid catalysts.

Introduction

Rare-earth compounds with organic complex cations are at present receiving attention¹ for their applications in organic synthesis² because rare-earth-mediated reactions display high chemical and stereo-selectivities. Among these materials, commercially available triflates have become the focus of much current research³ as recyclable water-tolerant Lewis acids catalysts used in mild conditions under organic or protic solvents, whose potentialities to substitute traditional strong Lewis acids have been much vaunted. Also, organolanthanide complexes have been reported to serve as highly efficient homogeneous catalysts in stereoselective intramolecular hydroamination/cyclization reactions.⁴ Environmental concerns have shifted, however, the attention to solid phase catalysts, with advantages such as adjusted reactivity, improved selectivity, simplified operation and separation methods, the possibility of recycling the catalysts, and eventually the reduction of hazardous pollution, playing thus a key role in the development of green chemistry. Like this, possible uses of trivalent lanthanide R^{3+} catalysts supported on ion exchange organic polymers (resins) have been studied for routine organic reactions.⁵ The design, the synthesis, and the

structure description of new compounds of the family of polymeric R-disulfonates $\text{R}(\text{OH})(\text{NDS})(\text{H}_2\text{O})$, $\text{R} = \text{Pr}, \text{Nd}$, $\text{NDS} = 1,5\text{-naphthalene disulfonate}$, which resulted in being highly operative as active and selective bifunctional catalysts in oxidation and epoxi ring opening, constitute one contribution of the authors in this field of research.⁶

On the other hand, apart from porous inorganic solid catalysts⁷ including well-known R-containing zeolites, widely used in acid-catalyzed processes in oil refining and the petrochemical industry, as well as in the production of fine and specialty chemicals,⁸ other solid compounds with inorganic complex anions⁹ have been scarcely investigated as possible catalysts¹⁰ in organic reactions. Taking advantage of the merits of both the behavior of R^{3+} and the solid phase in catalytic processes, as continuation of our previous work exploring the relation between structure and potential catalytic applications of R-containing ammonium double sulfates $\text{NH}_4\text{R}(\text{SO}_4)_2$, $\text{R} = \text{Nd}, \text{Eu}$,¹¹ we enlarge now the view over some of the remaining smaller R^{3+} cations, $\text{R} = \text{Y}, \text{Ho}$, for the same kind of organic reactions studied earlier. The catalytic hydrogenation of organic func-

* To whom correspondence should be addressed. E-mail ccascales@icmm.csic.es. Fax +34 913720623.

(1) Kagan, B. *Chem Rev.* **2002**, *102*, 1805.

(2) *Lanthanides: Chemistry and Use in Organic Synthesis*; Kobayashi, S., Ed.; Springer: Berlin, Germany, 1999.

(3) See, for example, Xie, W.; Jin, Y.; Wang, P. G. *CHEMTECH* **1999**, *29* (2), 23 and references therein. Waller, F. J.; Barrett, A. G. M.; Braddock, D. C.; McKinnell R. M.; Ramprasad, D. *J. Chem. Soc., Perkin Trans.* **1999**, *1*, 867. Matteucci, M.; Bhalay G.; Bradley, M. *Org. Lett.* **2003**, *5*, 235.

(4) Ryu, J. S.; Li, G. Y.; Marks, T. J. *J. Am. Chem. Soc.* **2003**, *125* (41), 12584.

(5) Yu, L.; Chen, D.; Li, J.; Wang, P. G. *J. Org. Chem.* **1997**, *62*, 3575.

(6) Snejko, N.; Cascales, C.; Gomez Lor, B.; Gutiérrez Puebla, E.; Iglesias, M.; Ruiz Valero, C.; Monge, M. A. *Chem. Commun.* **2002**, 1366.

(7) Wilson K.; Clark, J. D. *Pure Appl. Chem.* **2000**, *72* (7), 1313.

(8) Corma, A.; López Nieto, J. M. The use of rare-earth-containing zeolite catalysts. In *The Handbook on the Physics and Chemistry of Rare-Earths*, Gschneider, K. A., Eyring, L., Eds.; Elsevier Science B.V.: Amsterdam, The Netherlands, 2000; Vol. 29, p 269.

(9) Wickleder, M. S. *Chem. Rev.* **2002**, *102*, 2111, and references therein.

(10) Ouertani, M.; Girard, P.; Kagan, H. B. *Tetrahedron Lett.* **1982**, *23*, 4315. Lu, Z.-K.; Zu, W.-R. *Chin. J. Org. Chem.* **2000**, *20*, 819.

(11) Ruiz Valero, C.; Cascales, C.; Gómez Lor, B.; Gutiérrez Puebla, E.; Iglesias, M.; Monge, M.; Snejko, N. *J. Mater. Chem.* **2002**, *12*, 3073.

Table 1. Crystal Data and Structure Refinement for $\text{NH}_4\text{R}(\text{SO}_4)_2 \cdot \text{H}_2\text{O}$

empirical formula	$\text{NH}_4\text{Ho}(\text{SO}_4)_2 \cdot \text{H}_2\text{O}$	$\text{NH}_4\text{Y}(\text{SO}_4)_2 \cdot \text{H}_2\text{O}$
formula weight	393.05	317.03
crystal system	monoclinic	monoclinic
space group	$P2_1/n$	$P2_1/n$
<i>a</i> (Å)	10.2171(7)	10.219(2)
<i>b</i> (Å)	8.3349(5)	8.338(1)
<i>c</i> (Å)	10.3267(7)	10.323(2)
β (deg)	119.5290(10)	119.482(3)
volume (Å ³)	765.18(9)	765.7(2)
<i>Z</i>	4	4
density (calculated) ρ (Mg/m ³)	3.412	2.751
absorption coefficient μ /mm ⁻¹	10.915	8.191
<i>F</i> (000)	736	624
radiation	Mo K α (λ = 0.71073 Å)	Mo K α (λ = 0.71073 Å)
temperature (K)	296(2)	296(2)
diffractometer	Siemens Smart-CCD	Siemens Smart-CCD
crystal size (mm ³)	0.20 × 0.12 × 0.12	0.04 × 0.03 × 0.02
θ (deg) range for data collection	3.33 to 32.07	2.30 to 29.73
limiting indices (<i>h, k, l</i>)	(−6, −11, −15) to (15, 8, 5)	(−8, −11, −13) to (13, 8, 5)
reflections collected	3584	3133
independent reflections	1966	1658
<i>R</i> _{int}	0.0785	0.0966
absorption correction	SADABS	SADABS
goodness-of-fit on <i>F</i> ²	0.931	0.966
final <i>R</i> indices [<i>I</i> > 2 σ (<i>I</i>)]	<i>R</i> ₁ = 0.0373, <i>wR</i> ₂ = 0.0876	<i>R</i> ₁ = 0.0652, <i>wR</i> ₂ = 0.1266
<i>R</i> indices (all data)	<i>R</i> ₁ = 0.0509, <i>wR</i> ₂ = 0.0916	<i>R</i> ₁ = 0.1356, <i>wR</i> ₂ = 0.1519

tional groups is probably the most common application of heterogeneous catalysis in the synthesis of organic compounds.¹² The selective and rapid reduction of nitrocompounds is of continued interest in view of extensive synthetic applications. On the other hand, the selective oxidation of sulfides to sulfoxides has been a challenge for many years, partly due to the importance of sulfoxides as intermediates and auxiliaries in organic synthesis.¹³ In recent years selective oxidation of sulfides to sulfoxides has been carried out with a large number of heterogeneous and supported reagents.¹⁴

In this paper we report the synthesis, the crystal structure, and the catalytic use of Y- and Ho-ammonium sulfate materials in reactions of olefins hydrogenation and in hydrogen peroxide mediated oxidation of alkyl aryl sulfides to the corresponding sulfoxides. In hydrogenation reactions the catalytic properties have been contrasted with results obtained using a well-known rhodium organometallic catalyst,¹⁵ whereas for oxidation reactions the comparison is performed with activities of solid Ti-MCM41 and TS-1 catalysts.^{14d} Furthermore, current catalytic properties have also been compared with those previously reported¹¹ for larger Nd- and Eu-containing ammonium sulfates in the same organic reactions. The evaluation of these properties through several members of the R-series allows us to check the dependence for the catalytic activity on the R³⁺ metal center.

Experimental Section

Synthesis. The title compounds were synthesized hydrothermally from a reaction mixture containing $\text{R}(\text{NO}_3)_3 \cdot 6\text{H}_2\text{O}$

(R = Y or Ho) (0.8 g), propylamine (1 mL), dimethyl sulfoxide (14 mL), and HF (5 drops). The mixture was introduced and sealed in a Teflon-lined stainless steel autoclave and heated at 170 °C for 1 week under autogenous pressure, in each case, and cooled afterward. The corresponding solid products obtained were filtered and washed thoroughly with deionized water and acetone and then dried at room temperature.

Product Analyses. The purity of the above materials was checked from room temperature routinely carried out X-ray powder diffraction XRPD analyses (Siemens Kristalloflex 810 generator with Cu K α radiation source and a computer-controlled D-500 goniometer equipped with a graphite monochromator, scanning in steps of 0.02° 2 θ in the angular range of 5 ≤ 2 θ ≤ 60, with a counting time of 2 s each step), by comparison with corresponding simulated patterns on the basis of the single-crystal data. The IR spectra were recorded using pellets of sulfate samples dispersed in KBr, in the range 400–4000 cm⁻¹ on a Bruker ISS 66V-S spectrometer. Thermogravimetric and differential thermal TG-DT measurements were performed using a SEIKO TG/DTA 320U simultaneous thermal analyzer, under a nitrogen atmosphere (flow of 100 mL/min), heating from 26 to 700 °C at a rate of 5 °C/min.

X-ray Structure Determination. Suitable colorless (R = Y) or pink (R = Ho) single crystals with prismatic shape were mounted on a Siemens SMART CCD diffractometer equipped with a normal focus, 3-kW sealed tube. A summary of the fundamental crystal and refinement data for both compounds is given in Table 1. Data were collected at room temperature over a hemisphere of the reciprocal space by a combination of three sets of exposures. Each set had a different φ angle for the crystal and each exposure of 20 s covered 0.3° in ω . The crystal-to-detector distance was 5.09 cm. Unit cell parameters were determined by a least-squares fit of 60 reflections with *I* > 20 σ (*I*). Neutral-atom scattering factors for all atoms were used, and anomalous dispersion corrections were applied.¹⁶ All calculations were performed using the SHELXTL program.¹⁷ All the hydrogen atoms were located in the difference Fourier maps. Refinements were by full-matrix least-squares analyses with anisotropic thermal parameters for all non-hydrogen atoms and isotropic thermal parameters for hydrogen atoms.

Catalytic Experiments. (a) *Hydrogenation Experiments.* The catalytic properties of the title compounds in hydrogenation

- (12) Augustine, R. L. *Catal. Today* **1997**, 37, 419.
 (13) Drabowski, J.; Kilbasin, P.; Mikolajczyk, M.; *Synthesis of sulfoxides*; Wiley: New York, 1994.
 (14) (a) Kannan, P.; Sevel, R.; Rajagopal S.; Pitchumani, K. *Tetrahedron* **1997**, 53, 7635. (b) Hirano, M.; Yakabe, S.; Itoh, S.; Clark, J. H. *Synthesis* **1997**, 1161. (c) Hulea, C.; Moreau, P.; Di Renzo, F. *J. Mol. Catal. A* **1996**, 111, 355. (d) Corma, A.; Iglesias, M.; Sánchez, F. *Catal. Lett.* **1996**, 39, 153.
 (15) Corma, A.; Iglesias, M.; Molino, F.; Sánchez, F. *J. Organomet. Chem.* **1997**, 544, 147.

(16) *International Tables for Crystallography*; Kynoch Press: Birmingham, U.K., 1974; Vol. 4.

(17) *SHELXTL Version 6.10 Software Package*; Siemens Energy and Automation Inc. Analytical Instrumentation, 6300 Enterprise Lane, Madison, WI, 53719-1173, 1999.

Table 2. Atomic Coordinates ($\times 10^4$) and Equivalent Isotropic Displacement Parameters ($\text{\AA}^2 \times 10^3$)

	<i>x</i>	<i>y</i>	<i>z</i>	<i>U</i> (eq) ^a
Y/Ho	2802(1)/2804(1)	6395(1)/3607(1)	359(1)/361(1)	211(3)/9(1)
S(1)	6243(3)/6249(2)	6365(3)/3632(2)	1822(3)/1823(2)	226(6)/11(1)
S(2)	−1050(3)/1036(2)	7045(3)/7044(2)	−1009(3)/998(2)	226(6)/10(1)
O(1)	7030(9)/2961(7)	5650(9)/5660(7)	1092(8)/−1091(6)	29(2)/20(1)
O(2)	2370(9)/2380(6)	7848(9)/2167(7)	−1821(8)/−1818(6)	30(2)/20(1)
O(3)	5084(9)/5107(6)	7529(9)/2449(7)	784(8)/809(6)	27(2)/19(1)
O(4)	5382(9)/5379(7)	5157(9)/4841(6)	2134(9)/2121(6)	33(2)/20(1)
O(5)	−527(9)/523(8)	7872(9)/7891(7)	390(8)/−400(6)	31(2)/24(1)
O(6)	3266(9)/3289(7)	6818(8)/3186(6)	2747(8)/2752(6)	27(2)/16(1)
O(7)	2224(9)/2236(6)	4123(8)/5871(7)	1258(8)/1265(5)	27(2)/17(1)
O(8)	218(8)/232(7)	6228(8)/3775(6)	−1027(8)/−1020(7)	28(2)/20(1)
O(9)	2193(11)/2199(7)	9149(9)/842(7)	510(9)/513(6)	33(2)/19(1)
N	299(12)/4733(9)	6610(10)/8404(9)	3193(10)/1816(9)	34(2)/23(2)

^a *U*(eq) is defined as one-third of the trace of the orthogonalized \mathbf{U}^j tensor.

Table 3. Selected Bond Lengths (\AA) and Angles (deg) for $\text{NH}_4\text{Ho}(\text{SO}_4)_2 \cdot \text{H}_2\text{O}$, $\text{R} = \text{Y}, \text{Ho}^a$

Y/Ho—O(1)	2.331(7)/2.333(5)	O(8)—Y/Ho—O(6)	104.2(3)/104.6(2)	O(3)—Y/Ho—O(2)	71.3(3)/71.42(18)
Y/Ho—O(2)	2.397(7)/2.393(5)	O(8)—Y/Ho—O(7)	76.0(3)/76.2(2)	O(8)—Y/Ho—O(9)	81.0(3)/81.21(19)
Y/Ho—O(3)	2.394(7)/2.369(5)	O(6)—Y/Ho—O(7)	69.7(2)/69.68(18)	O(6)—Y/Ho—O(9)	73.0(3)/73.16(18)
Y/Ho—O(4)	2.573(9)/2.564(6)	O(8)—Y/Ho—O(1)	88.9(3)/88.6(2)	O(7)—Y/Ho—O(9)	129.1(2)/129.29(18)
Y/Ho—O(6)	2.298(7)/2.294(5)	O(6)—Y/Ho—O(1)	139.5(3)/139.2(2)	O(1)—Y/Ho—O(9)	147.6(3)/147.60(19)
Y/Ho—O(7)	2.311(7)/2.303(5)	O(7)—Y/Ho—O(1)	76.8(2)/76.70(19)	O(3)—Y/Ho—O(9)	82.4(3)/81.93(19)
Y/Ho—O(8)	2.307(8)/2.294(6)	O(8)—Y/Ho—O(3)	150.3(2)/150.42(19)	O(2)—Y/Ho—O(9)	69.2(2)/69.43(18)
Y/Ho—O(9)	2.404(7)/2.411(6)	O(6)—Y/Ho—O(3)	94.4(3)/93.47(19)	O(8)—Y/Ho—O(4)	151.2(2)/151.27(18)
S(1)—O(1)#2	1.472(7)/1.474(5)	O(7)—Y/Ho—O(3)	133.0(3)/132.77(19)	O(6)—Y/Ho—O(4)	72.5(2)/72.29(18)
S(1)—O(2)#1	1.460(8)/1.466(6)	O(1)—Y/Ho—O(3)	92.0(3)/92.75(19)	O(7)—Y/Ho—O(4)	76.1(3)/76.05(18)
S(1)—O(3)	1.499(8)/1.492(6)	O(8)—Y/Ho—O(2)	79.8(2)/79.95(19)	O(1)—Y/Ho—O(4)	77.9(3)/77.8(2)
S(1)—O(4)	1.474(7)/1.474(5)	O(6)—Y/Ho—O(2)	140.8(3)/141.13(19)	O(3)—Y/Ho—O(4)	56.9(2)/56.72(17)
S(2)—O(5)	1.445(7)/1.452(5)	O(7)—Y/Ho—O(2)	145.7(3)/145.8(2)	O(2)—Y/Ho—O(4)	121.5(2)/120.98(17)
S(2)—O(6)#3	1.467(7)/1.474(5)	O(1)—Y/Ho—O(2)	78.7(3)/78.56(19)	O(9)—Y/Ho—O(4)	123.0(3)/122.95(19)
S(2)—O(8)#4	1.467(8)/1.475(6)				
S(2)—O(7)	1.472(7)/1.484(6)				

^a Symmetry transformations used to generate equivalent atoms: (#1) $x + 1/2, -y + 1/2, z + 1/2$. (#2) $-x + 1, -y + 1, -z$. (#3) $-x + 1/2, y + 1/2, -z + 1/2$. (#4) $-x, -y + 1, -z$. (#5) $x - 1/2, -y + 1/2, z - 1/2$. (#6) $-x + 1/2, y - 1/2, -z + 1/2$.

tion reactions of hex-1-ene, cyclohexene, 1-methylcyclohexene, and nitroaromatics (nitrobenzene, 2-nitrophenol, 2-nitrofluorene, and 2-methyl-1-nitronaphthalene) were examined under conventional conditions for batch reactions in a reactor (Autoclave Engineers) of 100 mL capacity, at 40 °C, 4 atm dihydrogen pressure, and a metal/substrate molar ratio of 1/1000 for simple olefins and 1/100 for nitroaromatics. The results were monitored by gas liquid chromatography GLC using an internal standard reference. After hydrogenation, the catalyst was removed by filtration and used again.

(b) *Oxidation of Alkyl Aryl Sulfides.* The oxidation of methylphenylsulfide was carried out in a batch reactor at atmospheric pressure, using 1,2-dichloroethane as solvent (5 mL). Ten milligrams of the catalyst was stirred in a suspension containing the solvent and 1.0 mmol of the thioether. The oxidant, H_2O_2 , 30%, 3 mmol, was added dropwise, while the overall suspension was heated at 70 °C. Samples were taken at regular times and analyzed by GLC.

Results and Discussion

Crystal Structure Determination and Characterization. Upon determining the crystal structure, the composition was found to be $\text{NH}_4\text{R}(\text{SO}_4)_2 \cdot \text{H}_2\text{O}$, $\text{R} = \text{Y}, \text{Ho}$. Final atomic coordinates, bond distances, and bond angles are indicated in Tables 2 and 3.

These materials are isotopic with $\text{RbR}(\text{SO}_4)_2 \cdot \text{H}_2\text{O}^9$ and were previously synthesized only as polycrystalline powders.¹⁸ Eight oxygen atoms are surrounding the R ions, Figure 1, and the two independent sulfur atoms present the usual tetrahedral coordination, with distances and angles similar to those found⁹ in other sulfate compounds. Isolated RO_8 polyhedra are inter-

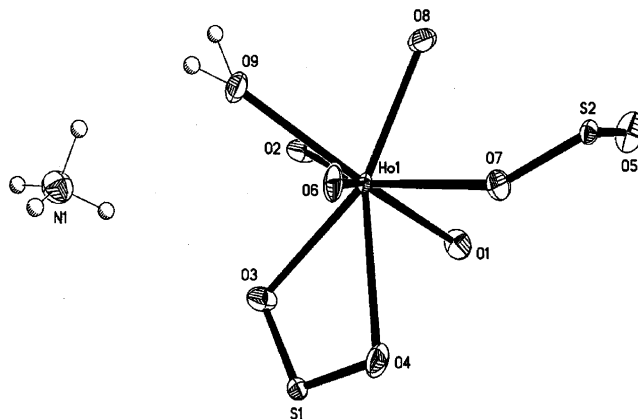


Figure 1. Labeled ORTEP plot of the asymmetric unit of $\text{NH}_4\text{Ho}(\text{SO}_4)_2 \cdot \text{H}_2\text{O}$.

connected through both S1 and S2 sulfate groups, Figures 2 and 3, with which they are sharing seven vertexes, and its remaining eighth oxygen, O9, belongs to a water molecule. Further, RO_8 polyhedra and S(1)- O_4 tetrahedra are sharing one edge, O3—O4, and therefore the distance R—S(1) (\AA) is only 3.069(3) and 3.072(2) for $\text{R} = \text{Y}, \text{Ho}$, respectively. Each S(1) O_4 tetrahedron is bridging four RO_8 polyhedra while S(2)- O_4 links three of these polyhedra, with its remaining oxygen free, being, as expected, the corresponding S(2)—O(5) distance the shorter one. These connections give rise to helical channels along the *a* direction, whose sequence is $-\text{RO}_8-\text{S}(2)\text{O}_4-\text{RO}_8-\text{S}(1)\text{O}_4-\text{RO}_8-\text{S}(2)\text{O}_4-\text{RO}_8-$, Figure 2, right. One ammonium cation per formula unit is needed to maintain the electrical neu-

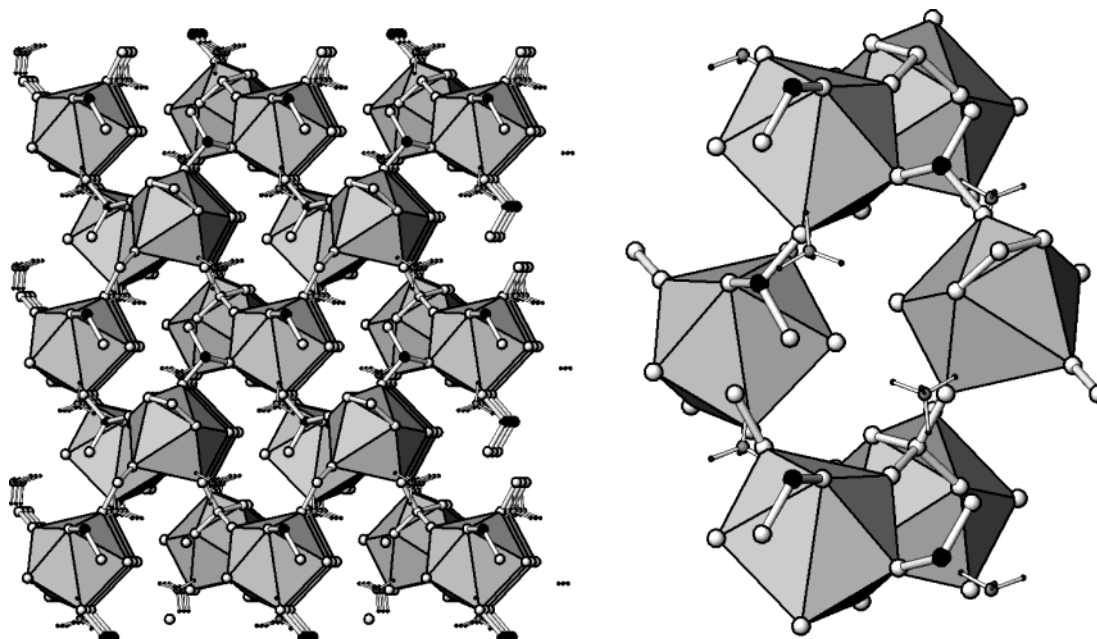


Figure 2. (a) *bc* view of the $\text{NH}_4\text{R}(\text{SO}_4)_2 \cdot \text{H}_2\text{O}$ structure, showing RO_8 polyhedra and S(1), light gray, and S(2), black, sulfate groups; (b) helical arrangement along the *a* direction, with NH_4^+ cations inside channels.

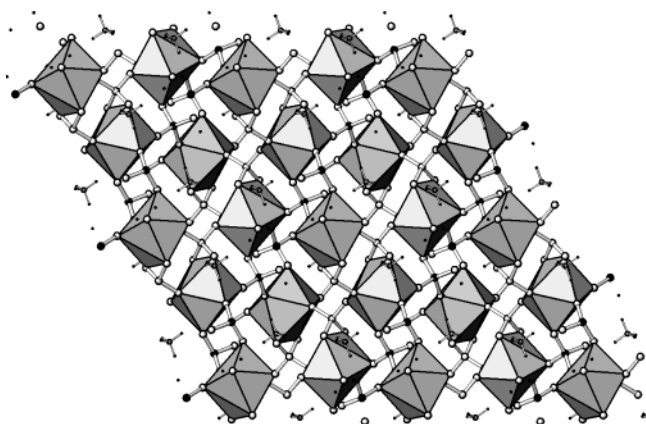


Figure 3. *ac* view of the $\text{NH}_4\text{R}(\text{SO}_4)_2 \cdot \text{H}_2\text{O}$ structure.

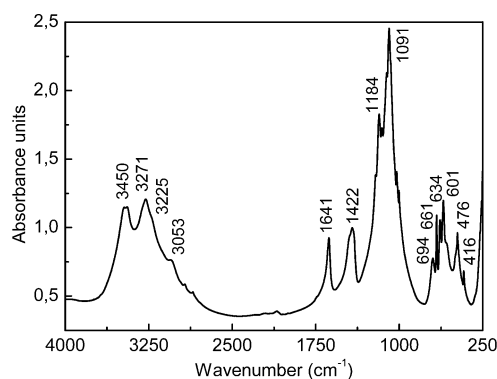


Figure 4. IR spectrum for $\text{NH}_4\text{Ho}(\text{SO}_4)_2 \cdot \text{H}_2\text{O}$.

trality. They are found inside the above helical channels. The positions of hydrogen atoms of this cation were also located. The NH_4^+ is bonded to different oxygen atoms of the framework through the four hydrogen atoms, two of them being in a bifurcated way, and the two others interacting with three oxygen atoms. Distances and angles from the nitrogen to the nearest oxygen atoms result in being characteristic of these arrangements.¹¹ Table 4 includes these distances as well as the hydrogen

Table 4. Bond Geometry (Å) and Angles (deg) for NH_4^+ in $\text{NH}_4\text{Ho}(\text{SO}_4)_2 \cdot \text{H}_2\text{O}$

N1–H11	1.08 (6)	N1–O3	2.89(1)
N1–H12	1.00 (6)	N1–O4	3.02(1)
N1–H13	0.86 (6)	N1–O5	2.79(1)
N1–H14	0.89 (6)	N1–O7	3.14(1)
H11···O2	1.99 (6)	N1–O8	3.10(1)
H11···O3	2.14 (6)	N1–O9	3.03(1)
H12···O1	2.63 (6)	N1–H11···O2	151 (1)
H12···O5	1.87 (6)	N1–H11···O3	124 (1)
H13···O3	2.80 (6)	N1–H12···O1	104 (1)
H13···O8	2.53 (6)	N1–H12···O5	151 (1)
H13···O9	2.70 (6)	N1–H13···O3	156 (1)
H14···O4	2.37 (6)	N1–H13···O8	125 (1)
H14···O5	2.50 (6)	N1–H13···O9	105 (1)
H14···O7	2.35 (6)	N1–H14···O4	131 (1)
N1–O1	3.03(1)	N1–H14···O5	100 (1)
N1–O2	2.99(1)	N1–H14···O7	143 (1)

bond geometry (N–H and H···O distances) and N–H···O angles for $\text{NH}_4\text{Ho}(\text{SO}_4)_2 \cdot \text{H}_2\text{O}$.

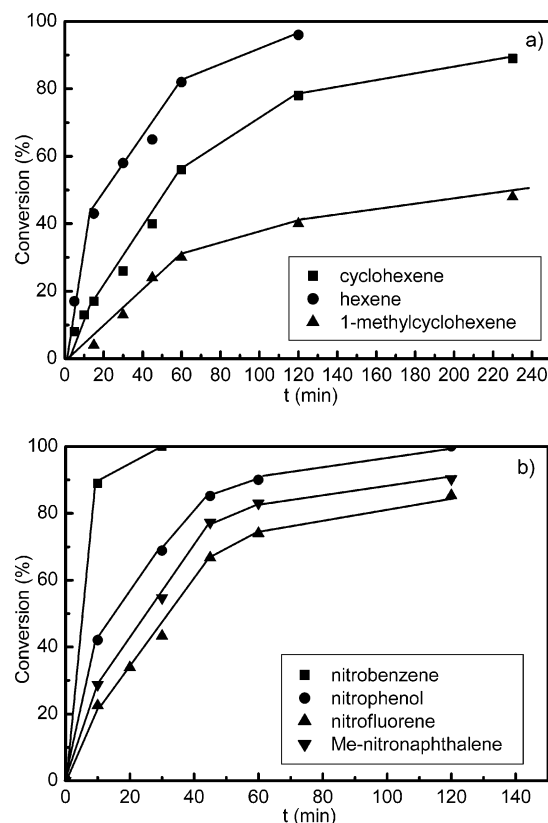
The infrared IR spectra of the title materials exhibit peaks at ≈ 3225 , ≈ 3050 , and $\approx 1420 \text{ cm}^{-1}$, characteristic of ν_3 , ν_1 , and ν_4 IR active NH_4^+ vibrations, respectively. For each compound, observed strong bands at 1090 – 1185 and 600 – 695 cm^{-1} correspond to ν_3 and ν_4 IR vibrations of the sulfate groups, whereas peaks with medium intensity at $\approx 475 \text{ cm}^{-1}$ can be assigned to the ν_2 vibration. The splitting found for ν_3 and ν_4 IR vibrations as well as the appearance in the IR spectra of the ν_2 Raman-active mode can be explained by assuming the lowering of the symmetry for the sulfate group. Finally, the existence of lattice water is consistent with absorption bands at 3270 – 3450 cm^{-1} (anti-symmetric and symmetric OH stretchings) and at 1640 cm^{-1} (HOH bending).¹⁹ Figure 4 corresponds to $\text{NH}_4\text{Ho}(\text{SO}_4)_2 \cdot \text{H}_2\text{O}$.

Thermogravimetric and differential thermal analyses carried out under N_2 indicate the loss of the coordination water upon heating to $\sim 150^\circ \text{C}$. Resulting anhydrous

(19) Nakamoto, K. *Infrared and Raman Spectra of Inorganic and Coordination Compounds*. John Wiley & Sons: New York, 1986.

Table 5. Hydrogenation of Alkenes Catalyzed by $\text{NH}_4\text{Ho}(\text{SO}_4)_2 \cdot \text{H}_2\text{O}$; Comparison with Other Catalysts

substrate	$\text{NH}_4\text{Ho}(\text{SO}_4)_2 \cdot \text{H}_2\text{O}$		$\text{NH}_4\text{Nd}(\text{SO}_4)_2$ (ref 11)	Rh-cat (ref 15)
	conversion (%) (min)	TOF ^a	TOF	TOF
hex-1-ene	100 (120)	4500	2900	5232
cyclohexene	80 (120)	1800	1245	3150
1-methylcyclohexene	40 (120)	800	700	312
nitrobenzene	100 (30)	1100	1000	2000
nitrophenol	90 (60)	450	350	600
2-nitrofluorene	75 (60)	280	140	400
2-methyl-1-nitronaphthalene	70 (60)	200	144	300

^a mmol of substrate/mmol of catalyst·min.**Figure 5.** Kinetic profile for (a) the hydrogenation of alkenes and (b) the reduction of nitroaromatics catalyzed by $\text{NH}_4\text{Ho}(\text{SO}_4)_2 \cdot \text{H}_2\text{O}$.

ammonium R-sulfates are stable at temperatures in the range 180–400 °C, before decomposing up to ~ 420 °C to the corresponding R-sulfates, which remain stable approaching the final measured temperature, 700 °C. Observed weight losses match exactly the described⁹ decomposition scheme.

Catalytic Activity. (a) *Hydrogenation Experiments.* Hex-1-ene, cyclohexene, and 1-methylcyclohexene were hydrogenated in the presence of $\text{NH}_4\text{Ho}(\text{SO}_4)_2 \cdot \text{H}_2\text{O}$ without an induction period, and isomerization was not detected, Figure 5. The maximum rate of hydrogenation of the three olefins resulted in the order hex-1-ene > cyclohexene > 1-methylcyclohexene. It seems that the enhanced surface concentration effect and/or an electrical interaction between the substrate and the material could indeed be responsible for the absence of an induction period. The turnover numbers are reported in Table 5.

The reduction of nitroaromatics proceeded with high yield and the turnover frequencies were in the range of 1100–200 min⁻¹, Table 5. The most important charac-

Table 6. Catalytic Properties of $\text{NH}_4\text{Ho}(\text{SO}_4)_2 \cdot \text{H}_2\text{O}$ in the Oxidation of Methylphenyl Sulfide; Comparison with Other Catalysts

catalyst	conversion (%) (min)	selectivity ^a (%)	TOF ^b	ref
$\text{NH}_4\text{Ho}(\text{SO}_4)_2 \cdot \text{H}_2\text{O}$	55 (180)	90	18	this work
none	5 (60)			this work
$\text{NH}_4\text{Nd}(\text{SO}_4)_2$	85 (180)	63	28	11
Ti-MCM ^c	80 (30)	76	24	14d
TS-1 ^c	29 (60)	79	10	14d

^a Amount of sulfoxide/amount of consumed sulfide. ^b mmol of substrate/mmol of catalyst·min. ^c Ti 2.5 wt %.

teristic of our catalytic system is the reduction of the bulky molecules as 2-nitrofluorene and 2-methyl nitronaphthalene in 100% yield within 2 h. The catalyst was recovered and reused without any reactivation, that is, retaining most of its catalytic activity at least four times. After each cycle the liquid phase was separated from the reaction mixture and examined for catalytic activity in the above hydrogenation of alkenes or nitroaromatics under the same conditions used with the solid catalyst. The results show that liquid phases are inactive for hydrogenation reactions. Moreover, these systems result in being significantly more stable than other homogeneous complexes, for example, the Rh-organometallic catalyst¹⁵ appearing in Table 5, that although shows higher activities, decomposes in the reaction media into Rh(0) particles, allowing thus prolonged reaction times, with no special care requirements in standard conditions.

When TOF values for each substrate are compared with those previously reported¹¹ for $\text{NH}_4\text{Nd}(\text{SO}_4)_2$ also included in the Table 5, they result in being considerably higher, and the difference in the catalytic activity using Ho or Nd-sulfates is getting lower when bulkier substrates are considered.

(b) *Oxidation of Alkyl Aryl Sulfides.* The described materials were tested as catalysts in the oxidation of organic substrates, using methylphenyl sulfide as the model substrate. The oxidation of methylphenyl sulfide was carried out in the presence of catalytic amounts of the title Ho compound (1% based on experimental metal content) by using hydrogen peroxide H_2O_2 as a sacrificial oxidant in CH_2Cl_2 at 70 °C. Higher reaction temperatures lead to a dramatic decrease in the selectivity to sulfoxide. Results from GC for the outcome of the reactions are summarized in Table 6. A series of blank experiments revealed that each component is essential for an effective catalytic reaction, and the system is proved to be relatively unaffected by changing the order of mixing. The catalyst appears to be stable under the experimental conditions, as after washing with CH_2Cl_2 the product recovered by filtration of the reaction

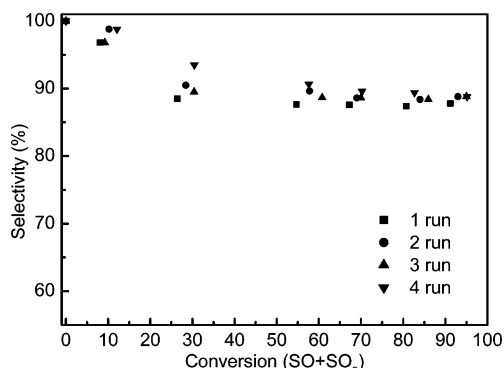


Figure 6. Selectivity to methylphenyl sulfoxide for the oxidation reaction after recycling the catalyst $\text{NH}_4\text{Ho}(\text{SO}_4)_2 \cdot \text{H}_2\text{O}$.

mixture continues showing its activity for further catalytic runs. Moreover, $\text{NH}_4\text{Ho}(\text{SO}_4)_2 \cdot \text{H}_2\text{O}$ compares well with other solid catalysts, i.e., Ti-zeolites, see Table 6, showing similar activity and chemoselectivity.

As indicated above, $\text{NH}_4\text{Ho}(\text{SO}_4)_2 \cdot \text{H}_2\text{O}$ can be reused at least four times without neither loss of selectivity, see Figure 6, nor activity with a catalyst loading as low as 1 mol %. Whereas the oxidation of the sulfide continued in the presence of $\text{NH}_4\text{Ho}(\text{SO}_4)_2 \cdot \text{H}_2\text{O}$, there is no further significant conversion when it is removed from the reaction system. Further, the same conclusion is independently confirmed by the absence of catalyst in the filtrate, determined from atomic absorption spectroscopy. On the other hand, $\text{NH}_4\text{Ho}(\text{SO}_4)_2 \cdot \text{H}_2\text{O}$ with an excess of oxidant and/or long times of reaction gives, as sole product, the corresponding sulfone with excellent yield.

The above selectivity curve shows that the sulfoxide is a primary and unstable product, while the corresponding sulfone appears as a secondary and stable product, although the oxidation to this final product evolves very slowly. The noteworthy qualitative difference with the reaction catalyzed by $\text{NH}_4\text{Nd}(\text{SO}_4)_2$ ¹¹ emerges from Figure 7. While for total conversions of the catalytic oxidation ranging below to ~45% similar amounts of sulfoxide result using both Nd and Ho catalysts, when the total conversion of the sulfide progresses, the sulfone yielded by the Nd-catalyzed oxidation became prevalent whereas with the Ho catalyst the product can still remain as a sulfoxide, with exceptionally low amounts of sulfone.

For all reactions tested with R-sulfate catalysts, a high selectivity in competitive reactions is observed for bulky substrates, which is correlated to structural effects (reactants size, selectivity effect). For Ho catalyst these good selectivities are associated with lower activities.

Although combinations of R^{3+} and H_2O_2 are among the most active systems for the hydrolysis of phosphodi-esters²⁰ and RNA,²¹ several problems associated with the low stability of $\text{R}^{3+}-\text{H}_2\text{O}_2$ mixtures as well as the

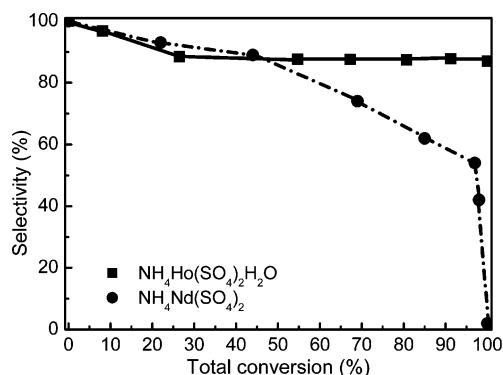


Figure 7. Comparison of selectivity curves to sulfoxide for the catalytic oxidation of methyl phenylsulfide.

tendency of R^{3+} to form polymeric species in aqueous solutions lead to discrepancies in the character of the active complexes.^{19,20} However, whatever is the nature of our active R-containing peroxosulfate catalytic complex, and beyond expected different reactivities related to the increasing electrostatic interaction for the smaller $\text{R}^{3+} = \text{Y}$, Ho cations, and thus their stronger ability to bind peroxide ligands, a clear correlation exists between the local environment of active R^{3+} metallic centers and the *selectivity* in oxidation reactions; that is, different structures of polymeric aggregates of the R-peroxosulfate suppose substantial variations of the rate of the oxidation reaction, depending on which sulfoxide or final sulfone will be obtained.

Conclusions

$\text{NH}_4\text{R}(\text{SO}_4)_2 \cdot \text{H}_2\text{O}$, $\text{R} = \text{Y}$, Ho, are catalytic systems tested in hydrogenation of olefins and in oxidation of organic sulfides. The combination of the advantages of the catalytic properties of R^{3+} centers and the solid phase, the required mild conditions of the carried out reactions, the possibility of recycling and reusing them with no detriment of selectivity, activity, or yield, qualify these materials as highly desirable catalysts for the development of environmentally benign processes. Moreover, in the above oxidation reactions they behave as highly selective catalysts to corresponding sulfoxides, in contrast with smaller R-containing ammonium sulfates $\text{NH}_4\text{R}(\text{SO}_4)_2$, $\text{R} = \text{Nd}$, Eu, which yield the over-oxidized sulfone.

Supporting Information Available: X-ray crystallographic files (CIF) for $\text{NH}_4\text{R}(\text{SO}_4)_2 \cdot \text{H}_2\text{O}$, $\text{R} = \text{Y}$, Ho. This material is available free of charge via the Internet at <http://pubs.acs.org>.

CM049347H

(20) Mejia-Radillo, Y.; Yatsimirsky, A. *Inorg. Chim. Acta* **2002**, 328, 241, and references therein.

(21) Kamitani, J.; Sumaoka, J.; Asanuma, H.; Komiyama, M. *J. Chem. Soc., Perkin Trans.* **1998**, 2, 523.